

Vector boson scattering in CMS

Meng Lu^a on behalf of the CMS Collaboration

^a*Sun Yat-Sen University,
GuangZhou, China*

E-mail: meng.lu@cern.ch

Vector boson scattering is a key production process to probe the electroweak symmetry breaking of the standard model, since it involves both self-couplings of vector bosons and coupling with the Higgs boson. If the Higgs mechanism is not the sole source of electroweak symmetry breaking, the scattering amplitude deviates from the standard model prediction at high scattering energy. Moreover, deviations may be detectable even if a new physics scale is higher than the reach of direct searches. Latest measurements of production cross sections of vector boson pairs in association with two jets in proton-proton collisions at $\sqrt{s} = 13$ TeV at the LHC are reported using a data set recorded by the CMS detector. Differential fiducial cross sections as functions of several quantities are also measured.

*** *The European Physical Society Conference on High Energy Physics (EPS-HEP2021), ****

*** *26-30 July 2021 ****

*** *Online conference, jointly organized by Universität Hamburg and the research center DESY ****

1. Introduction

The standard model (SM) has been well tested and becomes complete after the discovery of Higgs boson in the ATLAS [1, 2] and CMS [3–5] experiment. The properties of Higgs boson, e.g., its coupling with vector bosons and fermions and the mass of Higgs boson, are vital for us to have a better understanding of Higgs boson and the Higgs mechanism, the latter one is of great importance as it provides masses for those massive particles. We know that three of the Goldstone Higgs bosons are eaten by the massless gauge bosons and become the longitudinal polarized component of the gauge bosons during the spontaneous symmetry breaking (SSB), which make the gauge bosons become massive. Inspired by the procedure how massive bosons obtain mass, we could study the SSB through the vector boson scattering (VBS), in which the longitudinal polarized VBS is the most interesting and important.

The typical topology of VBS is shown in Fig. 1. Two vector bosons are radiated from the initial state quarks and directly interact via scattering to produce a final state of two scattered vector bosons and two jets (VBS jets) from the quarks. The VBS processes have unique topologies as listed below:

- the VBS jets tend to be back-to-back, thus have very large separation in pseudorapidity.
- the invariant mass of two VBS jets is large, could reach TeV scale
- low hadronic activities in the central region

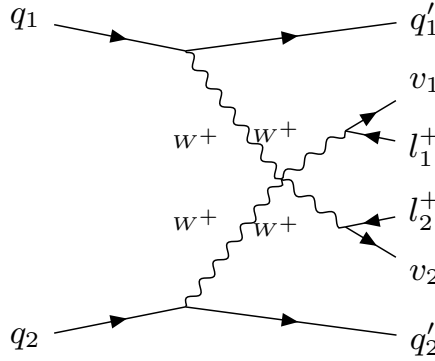


Figure 1: Scattering between two same sign charged W bosons with leptonic decays.

Besides the ability of SSB study, the VBS processes could also be used to search physics beyond SM (BSM) by introducing operators stands for anomalous couplings which are not allowed in SM, e.g., the coupling between four Z bosons. The extended lagrangian reads:

$$\mathcal{L}_{\text{eff}} = \mathcal{L}_{\text{SM}} + \sum_{n=5}^{\infty} \frac{f_n}{\Lambda^{n-4}} \mathcal{O}_n \quad (1)$$

where \mathcal{L}_{SM} is the lagrangian of SM, and f_n , Λ^{n-4} , \mathcal{O}_n are the coefficient, the energy scale and the anomalous operator with dimension n, respectively. The VBS processes are pure EW at leading order (LO) which are predicted by the SM precisely, thus they are sensitive to potential BSM which may promote the production of VBS events. The CMS collaboration has performed comprehensive measurements on the VBS processes, several recent measurements will be introduced in this article.

27 2. VBS WV

28 VBS WV [6] is a semi-leptonic channel, where “V” can be a Z boson or W boson which decay
 29 hadronically. This semi-leptonic decay channel has larger cross section than fully leptonic decay
 30 channel, and has smaller backgrounds than fully hadronic decay channel. The final states contain
 31 two VBS jets, two jets from vector boson (V-jets), one lepton and missing transverse momentum
 32 (MET). The separation between two V-jets depends on the energy of the hadronically decaying
 33 vector boson, thus the final states could be assigned to two categories, i.e., the boosted and the
 34 resolved. The two V-jets will be reconstructed as a single jet with large cone size (cone = 0.8),
 35 which refer to as AK8 jet. In the resolved case, two jet with small cone size 0.4 (AK4 jet) will be
 36 reconstructed. In both cases, the VBS jets are reconstructed with cone size 0.4. It’s obvious that
 37 invariant mass of either the AK8 jets or of two AK4 V-jets should be close to the mass of W/Z
 38 boson. The definitions of signal region (SR) together with several other control regions (CR) are
 summarized in Fig. 2.

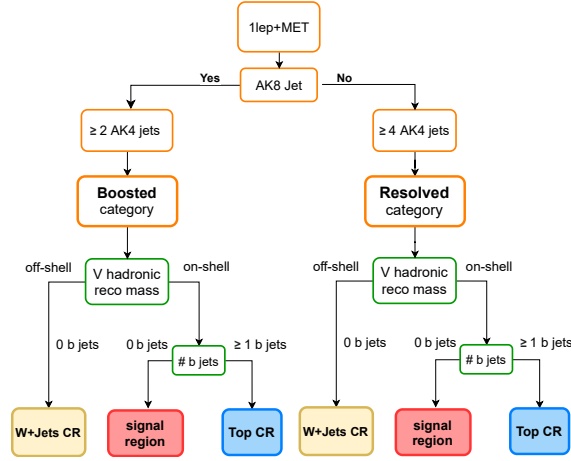


Figure 2: Analysis workflow: objects and categories selection followed by control regions (CR) and signal regions definition [6].

39 DNN method is used to separate signal and all the other backgrounds. Different DNNs
 40 are used for resolved and boosted case. The signal extraction is performed in several different
 41 signal definitions. The measurement of the purely EW signal strength μ_{EW} keeping the QCD WV
 42 production contribution fixed to the SM prediction $\mu_{QCD} = 1$, the measurement of the signal strength
 43 considering as signal the EW and QCD WV processes together, and finally a 2D simultaneous
 44 measurement of the signal strengths μ_{EW} and μ_{QCD} . The observed electroweak signal strength is:

$$\mu_{EW} = \sigma^{\text{obs}} / \sigma^{\text{SM}} = 0.85^{+0.24}_{-0.20} = 0.85^{+0.21}_{-0.17} (\text{syst})^{+0.12}_{-0.12} (\text{stat}), \quad (2)$$

46 $(1^{+0.24}_{-0.22}$ expected), where σ^{obs} and σ^{SM} are the observed and predicted cross section respectively,
 47 corresponding to an observed evidence for the SM signal at 4.4 standard deviations, 5.1 expected.

48 Considering instead the signal as the overall EW and QCD WV production, the signal strength
 49 $\mu = \sigma^{\text{obs}} / \sigma^{\text{SM}}$ is measured to be:

$$\mu_{EW+QCD} = \sigma^{\text{obs}} / \sigma^{\text{SM}} = 0.98^{+0.20}_{-0.17} = 0.98^{+0.19}_{-0.16} (\text{syst})^{+0.07}_{-0.07} (\text{stat}), \quad (3)$$

($1_{-0.18}^{+0.19}$ expected) corresponding to a cross section defined in the same fiducial phase space as the pure EW one of $16.6_{-2.9}^{+3.4}$ pb, $16.9_{-2.1}^{+2.9}$ (scale) $_{-0.5}^{+0.5}$ (pdf) expected.

3. VBS same sign WW and WZ

This is a combined analysis including VBS same sign WW (ssWW) and WZ [7], in both channels the vector boson decay leptonically. With the knowledge from previous studies, we know that ssWW is a very clean channel that the EW component dominates over the QCD-induced component in the signal region. A sequential selection is used in ssWW channel to perform the signal extraction. A BDT method is used to separate signal and backgrounds for the VBS WZ channel. The significance of the EW WZ signal is quantified from the p value using a profile ratio test statistic and asymptotic results for the test statistic. The observed (expected) statistical significance of the EW WZ signal is 6.8 (5.3) standard deviations, while the statistical significance of the EW $W^{\pm}W^{\pm}$ signal is far above 5 standard deviations.

Inclusive fiducial cross section measurements for the EW $W^{\pm}W^{\pm}$, EW+QCD $W^{\pm}W^{\pm}$, EW WZ, QCD WZ, and EW+QCD WZ processes and the theoretical predictions are summarized in Tab. 1. The measurements are more consistent with theoretical predictions without next-to-LO (NLO) corrections. Besides the inclusive cross section measurements, differential cross sections are also performed with respect to the m_{jj} and $m_{\ell\ell}$ for both VBS ssWW and VBS WZ.

The events in the ssWW and WZ SRs are used to constrain anomalous quartic gauge boson coupling (aQGC) in the effective field theory (EFT) framework. The diboson transverse mass are used for this study and no obvious deviation is found, a set of limits are obtained on the anomalous operators.

Table 1: The measured inclusive fiducial cross sections for the EW $W^{\pm}W^{\pm}$, EW+QCD $W^{\pm}W^{\pm}$, EW WZ, EW+QCD WZ, and QCD WZ processes and the theory predictions with MADGRAPH5_AMC@NLO at LO. The EW processes include the corresponding interference contributions. The theoretical uncertainties include statistical, PDF, and scale uncertainties. Predictions with applying the $O(\alpha_S\alpha^6)$ and $O(\alpha^7)$ corrections to the MADGRAPH5_AMC@NLO LO cross sections, as described in the text, are also shown. The predictions of the QCD $W^{\pm}W^{\pm}$ and WZ processes do not include additional corrections. All reported values are in fb [7].

Process	$\sigma_{\mathcal{B}}$ (fb)	Theory prediction (fb)	Theory prediction with NLO corrections (fb)
EW $W^{\pm}W^{\pm}$	3.98 ± 0.45	3.93 ± 0.57	3.31 ± 0.47
	0.37 (stat) \pm 0.25 (syst)		
EW+QCD $W^{\pm}W^{\pm}$	4.42 ± 0.47	4.34 ± 0.69	3.72 ± 0.59
	0.39 (stat) \pm 0.25 (syst)		
EW WZ	1.81 ± 0.41	1.41 ± 0.21	1.24 ± 0.18
	0.39 (stat) \pm 0.14 (syst)		
EW+QCD WZ	4.97 ± 0.46	4.54 ± 0.90	4.36 ± 0.88
	0.40 (stat) \pm 0.23 (syst)		
QCD WZ	3.15 ± 0.4	3.12 ± 0.70	3.12 ± 0.70
	0.45 (stat) \pm 0.18 (syst)		

71 4. Longitudinal polarized ssWW

72 As we have discussed in the introduction, the longitudinal polarized component of vector boson
 73 is related to the Higgs mechanism. Though the scattering between longitudinal polarized vector
 74 has been pursued for a long time, it is not possible until the ATLAS and CMS experiments collect
 75 large amount of data. CMS collaboration performed the first study on longitudinal polarized VBS
 76 through ssWW channel [8]. In the ssWW channel, each of the W bosons can be polarized either
 77 longitudinally (W_L) or transversely (W_T), leading to three distinct contributions $W_L^\pm W_L^\pm$, $W_L^\pm W_T^\pm$ and
 78 $W_T^\pm W_T^\pm$. But due to limited data sample size, two measurements are performed: one for $W_L^\pm W_L^\pm$ and
 79 $W_X^\pm W_T^\pm$; and another for $W_L^\pm W_X^\pm$ and $W_T^\pm W_T^\pm$. The index X indicates either of the two polarization
 80 states. Such study is very challenge due to the fact that the VBS processes have very small cross
 81 section, and the contribution of longitudinal component is only around 10 percent of the inclusive
 82 VBS process. The other challenge is due to kinematic similarity between different polarized VBS
 83 components. Trigger by this difficulty, a multi-variable analysis method is used to separate different
 84 polarized components, and to separate VBS and other backgrounds.

85 Since the definition of polarization depends on the choice of reference frame, the measurements
 86 are performed in two different reference frames, e.g., the WW center-of-mass and the initial-state
 87 parton-parton reference frames. The observed (expected) significance of $W_L^\pm W_L^\pm$ component in
 88 WW reference frame is 2.3 (3.1) standard deviations, while the observed (expected) significance
 89 in parton-parton reference frames is 2.6 (2.9) standard deviations. The cross section of different
 90 definition of signals are listed in Table. 2. In general, the measurements are consistent with the
 theoretical prediction within uncertainties.

Table 2: Measured fiducial cross sections for the $W_L^\pm W_L^\pm$ and $W_X^\pm W_T^\pm$ processes and for the $W_L^\pm W_X^\pm$ and $W_T^\pm W_T^\pm$ processes for the helicity eigenstates defined in the $W^\pm W^\pm$ center-of-mass frame. The theoretical predictions including the $O(\alpha_S \alpha^6)$ and $O(\alpha^7)$ corrections to the MADGRAPH5_AMC@NLO LO cross sections, as described in the text, are also shown. The theoretical uncertainties include statistical, PDF, and LO scale uncertainties. \mathcal{B} is the branching fraction for $WW \rightarrow \ell\nu\ell'\nu$ [9].

Process	$\sigma \mathcal{B}$ (fb)	Theoretical prediction (fb)
$W_L^\pm W_L^\pm$	$0.32^{+0.42}_{-0.40}$	0.44 ± 0.05
$W_X^\pm W_T^\pm$	$3.06^{+0.51}_{-0.48}$	3.13 ± 0.35
$W_L^\pm W_X^\pm$	$1.20^{+0.56}_{-0.53}$	1.63 ± 0.18
$W_T^\pm W_T^\pm$	$2.11^{+0.49}_{-0.47}$	1.94 ± 0.21

92 5. VBS $Z\gamma$

93 Different from the massive VBS process, the VBS $Z\gamma$ [10] is not able to study the Higgs
 94 mechanism due to that photon does not directly couple to the Higgs boson. The interests of VBS
 95 $Z\gamma$ is its sensitivity to pure neutral aQGCs, i.e., $ZZZ\gamma/ZZ\gamma\gamma/Z\gamma\gamma\gamma$. This analysis focuses on the
 96 leptonic decay channel, thus the final state contains two electrons or two muons with invariant mass

97 within Z mass window, one photon and two VBS jets. The events are categorized to four channels,
98 i.e., muon (electron) + photon in barrel (endcap) region.

99 The main backgrounds are the QCD-induced $Z\gamma$ and those processes with same final states
100 but the photon are not prompt. The contribution of QCD-induced $Z\gamma$ is directly estimated using
101 simulation. The contribution of nonprompt backgrounds are estimated using data-driven method,
102 i.e., performing fit on the shape of σ_{ieie} of photon, while σ_{ieie} stands for the centrality of the
103 photon energy deposit on the detector. The EW signal extraction is performed by a simultaneous
104 fit between signal region and control region through a two dimensional distribution of m_{jj} and $\Delta\eta_{jj}$.
105 The observed significance of the EW signal is much higher than 5 standard deviations. The best fit
106 value for the EW $Z\gamma$ signal strength and the measured fiducial cross section are

$$\begin{aligned}\mu_{EW} &= 1.20^{+0.12}_{-0.12}(\text{stat})^{+0.14}_{-0.12}(\text{syst}) \\ &= 1.20^{+0.18}_{-0.17}\end{aligned}\quad (4)$$

$$\begin{aligned}\sigma_{EW}^{\text{fid}} &= 5.21 \pm 0.52(\text{stat}) \pm 0.56(\text{syst})\text{fb} \\ &= 5.21 \pm 0.76\text{fb}\end{aligned}\quad (5)$$

108 The best fit value for the combined $Z\gamma jj$ signal strength and the measured fiducial cross section are

$$\begin{aligned}\mu_{EW+QCD} &= 1.11^{+0.06}_{-0.06}(\text{stat})^{+0.10}_{-0.09}(\text{syst}) \\ &= 1.11^{+0.12}_{-0.11}\end{aligned}\quad (6)$$

$$\begin{aligned}\sigma_{EW+QCD}^{\text{fid}} &= 14.7 \pm 0.80(\text{stat}) \pm 1.26(\text{syst})\text{fb} \\ &= 14.7 \pm 1.53\text{fb}\end{aligned}\quad (7)$$

110 The theoretical fiducial cross section for the EW $Z\gamma$ signal at LO accuracy is $4.34 \pm 0.26(\text{scale}) \pm$
111 $0.06(\text{PDF})\text{fb}$, and the expected fiducial cross section for the combined QCD and EW $Z\gamma jj$ pro-
112 duction is $13.3 \pm 1.72(\text{scale}) \pm 0.10(\text{PDF})\text{fb}$. Besides the inclusive cross section measurements,
113 differential cross section measurements are also derived on with respect to the p_T of leading lepton,
114 leading jet and photon, as well as on the invariant mass of two jets. In general, good agreements
115 are obtained between measurements and theoretical predictions. The invariant mass of Z boson
116 and photon is used for aQGC study, no obvious deviation from SM is found thus a set of limits are
117 obtained.

118 6. VBS $W\gamma$

119 Similar with VBS $Z\gamma$, the main motivation of VBS $W\gamma$ [11] is its sensitivity to aQGCs.
120 Different from the several analysis introduced above, this analysis use the data collected in 2016
121 which corresponds to a integrated luminosity 35.9fb^{-1} . The main backgrounds of this channel
122 are the QCD-induced $W\gamma$, nonprompt photon and nonprompt lepton. The contribution of QCD-
123 induced $W\gamma$ is estimated using simulation, and the contribution of nonprompt backgrounds are
124 derived using the methods introduced above. The EW signal extraction uses the similar strategy
125 with VBS $Z\gamma$, i.e., perform simultaneous fit between signal region and control region with respect
126 to invariant mass of two jets m_{jj} , and invariant mass of lepton and photon $m_{\ell\gamma}$. The observed
127 (expected) significance of EW signal is 4.9 (4.6) standard deviations using 2016 data, while 5.3

128 (4.8) standard deviations is obtained after combining with data collected in 2012 [12]. This is the
 129 first observation of VBS $W\gamma$. The signal strength and corresponding fiducial cross section of EW
 130 signal are

$$\mu_{EW} = 1.20^{+0.26}_{-0.24} \quad (8)$$

$$\sigma_{EW}^{\text{fid}} = 20.4 \pm 0.4(\text{lumi}) \pm 2.8(\text{stat}) \pm 3.5(\text{syst}) \text{ fb} = 20.4 \pm 4.5 \text{ fb} \quad (9)$$

132 for the EW+QCD signal, the signal strength and corresponding fiducial cross section are

$$\mu_{EW+QCD} = 1.21^{+0.17}_{-0.16} \quad (10)$$

$$\sigma_{EW+QCD}^{\text{fid}} = 108 \pm 2(\text{lumi}) \pm 5(\text{stat}) \pm 15(\text{syst}) \text{ fb} = 108 \pm 16 \text{ fb} \quad (11)$$

134 The invariant mass of W boson and photon is used for aQGC study. No obvious deviation from SM
 135 is found and a set of limits are obtained. These are the most stringent limits to date on the aQGC
 136 parameters $f_{M,2-5}/\Lambda^4$ and $f_{T,6-7}/\Lambda^4$.

137 7. Summary

138 The CMS collaboration has performed comprehensive studies of the vector boson scattering
 139 process, containing massive vector boson scattering as well as those with photon, most of them are
 140 performed with data collected from 2016 to 2018, which corresponding to a integrated luminosity
 141 137 fb^{-1} . The first measurement of longitudinal polarized vector boson scattering is performed
 142 through same sign WW channel. Vector boson scattering processes could be used to search physics
 143 beyond standard model by introducing anomalous couplings between vector bosons. Several works
 144 have implement such study and no obvious deviation from standard model is found, which lead to
 145 a set of limits on the anomalous couplings.

146 **References**

- 147 [1] ATLAS Collaboration, “The ATLAS Experiment at the CERN Large Hadron Collider”, JINST
148 3 S08003 (2008)
- 149 [2] ATLAS Collaboration, “Observation of a new particle in the search for the standard model
150 Higgs boson with the ATLAS detector at the LHC”, Phys. Lett. B, 716:1, (2012)
- 151 [3] CMS Collaboration, “The CMS experiment at the CERN LHC”, JINST 3 S08004 (2008)
- 152 [4] CMS Collaboration, “Observation of a new boson at a mass of 125 GeV with the CMS
153 experiment at the LHC”, Phys. Lett. B, 716:30, (2012)
- 154 [5] CMS Collaboration, “Observation of a new boson with mass near 125 GeV in pp collisions at
155 $\sqrt{s} = 7$ and 8 TeV”, J. High Energy Phys., 06 (2013) 081
- 156 [6] CMS Collaboration, “Search for vector boson scattering at the LHC Run 2 with CMS data in
157 the semi-leptonic $lvqq$ final state”, <http://cds.cern.ch/record/2776799?ln=en/>
- 158 [7] CMS Collaboration, “Measurements of production cross sections of WZ and same-sign WW
159 boson pairs in association with two jets in proton-proton collisions at $\sqrt{s} = 13$ TeV”, Physics
160 Letters B, 809:135710, 2020.
- 161 [8] CMS Collaboration, “Measurements of production cross sections of polarized same-sign W
162 boson pairs in association with two jets in proton-proton collisions at $\sqrt{s} = 13$ TeV”, Physics
163 Letters B, 812:136018, (2021)
- 164 [9] Particle Data Group and M. Tanabashi and others, “Review of particle physics”, Phys. Rev. D,
165 98:030001, (2018).
- 166 [10] CMS Collaboration, “Measurement of the electroweak production of $Z\gamma$ and two jets in proton-
167 proton collisions at $\sqrt{s} = 13$ TeV and constraints on anomalous quartic gauge couplings”,
168 Phys. Rev. D. 809, (2021).
- 169 [11] CMS Collaboration, “Observation of electroweak production of $W\gamma$ with two jets in proton-
170 proton collisions at $\sqrt{s} = 13$ TeV”, Physics Letters B. 811, (2020).
- 171 [12] CMS Collaboration, “Measurement of electroweak-induced production of $W\gamma$ with two jets in
172 pp collisions at $\sqrt{s} = 8$ TeV and constraints on anomalous quartic gauge couplings”, J. High
173 Energ. Phys. 2017, 106 (2017).